Needle localization for needle steering under 3D ultrasound feedback*

Guillaume Lapouge[1,2], Jocelyne Troccaz[1], Philippe Poignet[2]

***Abstract*— In needle steering, estimating the needle pose is a critical problem. In 3D ultrasound volumes, fine needle localization is difficult and requires a combination of estimation and image processing to be successful. Indeed, 3D ultrasound imaging suffers from noise, artifacts and works at a low frequency. We propose a needle tip pose estimation method in the context of 3D robotic needle steering under 3D ultrasound feedback, based on multi-rate, multi-sensor fusion [1].**

I. Introduction

In surgery, the success of percutaneous operations seems closely related to the precision of the procedure. To increase the procedure efficacy, robotic needle steering has been extensively researched. Needle steering requires feedback for closed loop control of a flexible needle. This feedback consists, most of the time, in ultrasound (US) imaging for its ease of use despite the quality of the acquired images.

3D robotic needle steering has been validated with camera-based feedback in [2]. In the context of clinically-compatible US feedback, most solutions (i.e. [4], [5] and [6]) involve the translation of a 2D probe used in B-mode imaging to follow the needle tip during the insertion. This feedback is referred to as 2.5D US imaging. It aims at solving the poor needle detection in the ultrasound images by putting a 2D, 25 Hz US probe in position of needle maximal visibility (i.e. orthogonal to the needle shaft). Such a feedback makes the needle localization easier but may prove difficult to transpose to a clinical use. Indeed, the translation of the probe requires an external device and might cause unwanted tissue deformation.

3D US probes seem more adapted to a clinical use than their 2D counterparts. However, their low framerate (around 1 Hz) and low image quality represent a challenge for precise needle localization.

A. 3D US probe used in Doppler mode

3D US imaging set in Doppler mode has been used in [7]. In this study, the needle is vibrated with an external device. The vibrations are then detected by the probe and the needle is defined as the curve that best fits the doppler patches in the volume. The clinical application of such a method seems however difficult for security and practical reasons.

A method without need for vibrations has been developed in [8]. In this study, the needle is rotated during the acquisition, this rotation is then detected in Doppler mode. However, the precision of this method is low despite additional constraints put on the needle insertion.

Doppler mode for needle steering seems adequate when the needle is not visible in B-mode images. However, it requires additional constraints which may prove difficult to transpose to a clinical application.

B. 3D US probe used in B-mode

Needle steering under 3D US B-mode imaging has very rarely be developed. The reason lies in the difficulty to detect fine needles in volumes that are noisy, acquired at 1 Hz and suffer from many artifacts. Besides, analysing the entire 3D US volume would be computationally too costly.

In [9] the needle is kept in a position of best visibility by guiding the ultrasound probe with a robot. The needle position is estimated by a Kalman filter which will also provide a region of interest (ROI) for the next segmentation. Inside this ROI, and after an intensity-based voxel binarisation, a RANSAC algorithm fits a Bezier curve to the resulting 3D data. This method was augmented with particle filtering in [10]. However, the needle is manually inserted in this study and no information about insertion speed and rotation is taken into account. In [11], we described a Kalman filter based on a mechanical model and fed by the robot inputs. This filter provides a ROI for the needle localization. The needle is then detected similarly to the method mentioned before. A laser microetching of the needle roughens its surface for more echogenicity. However, the needle maximum curvature is considered constant throughout the insertion which may not be the case in clinical applications.

II. Contribution

A. Methods

To increase the quality of the needle tip pose estimation, we propose to take into account asynchronous multi-sensor measurements. To do so, a multi-rate unscented Kalman filtering (as presented in [12]) is proposed. This filter will take into account measurements coming from 3D B-mode US imaging, from the robot sensors and from shear wave elasticity imaging (SWE) (cf. Figure 1).

The needle tip-tissue interaction is modelled by the bicycle model first introduced in [13] and under the form

$$\begin{bmatrix} \dot{x} \\ y \\ z \\ \alpha \\ \beta \\ \gamma \\ \kappa \end{bmatrix} = \begin{bmatrix} \cos\alpha\cos\beta & 0 \\ \sin\beta & 0 \\ \cos\beta\sin\alpha & 0 \\ \kappa\cos\gamma\sec\beta + \kappa\frac{\beta_{cut}}{2}\sin\gamma\cos\gamma\tan\beta & -\frac{\beta_{cut}}{2}\sin\gamma \\ \kappa\sin\gamma - \kappa\frac{\beta_{cut}}{2}\cos\gamma\cos\gamma\tan\beta & \frac{\beta_{cut}}{2}\cos\gamma \\ -\kappa\cos\gamma tan\beta & 1 \\ 0 & 0 \end{bmatrix} \begin{bmatrix} u_1 \\ u_2 \end{bmatrix} \quad (1)$$

*This work was partly supported by the Investissements d'Avenir programme (Labex CAMI) under reference ANR-11-LABX-0004

[1]Univ. Grenoble Alpes, CNRS, Grenoble INP, TIMC-IMAG, F-38000 Grenoble, France

[2]Univ. Montpellier, CNRS, LIRMM, F-34090 Montpellier, France
guillaume.lapouge@univ-grenoble-alpes.fr

where x, y and z are the Cartesian coordinates of the needle tip in the 3D US volume frame [mm]; α, β and γ are the yaw, pitch and roll of the needle tip [rad]; κ is the curvature of the needle tip trajectory [mm^{-1}]. The inputs u_1 and u_2 correspond to the insertion speed [$mm.s^{-1}$] and the rotation speed [$rad.s^{-1}$] of the needle tip respectively. β_{cut} is the cutting angle detailed in [15].

SWE provides a measurement of tissues stiffness under small deformations. The stiffer the medium is, the smaller the radius of curvature of the needle path is [4]. Therefore, SWE measurements can be considered as curvature measurements. Each needle was inserted into phantoms of different stiffnesses to establish relationship between needle curvature and tissue elasticity. A power curve is then fitted to the data resulting in the following equation: $\kappa = aE^b$, with κ the needle curvature, E the tissue Young's modulus and a, $b \in \mathbb{R}^2$.

Because $\kappa \cos\gamma tan\beta$ is most of the time small, $\dot{\gamma} \approx u_2$ and the needle base rotation measured by the robot can be considered as a measurement of the tip roll angle γ. Needle tip segmentation in 3D B-mode US volumes provides a measurement of the Cartesian coordinates of the tip in the US volume frame.

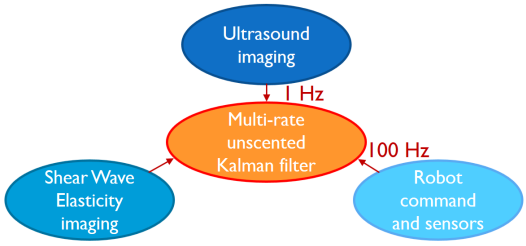

Fig. 1. Proposed structure of the multi-rate unscented Kalman filter. Data flows are represented by arrows. Refresh rates are indicated in red when specifiable.

The measurement equation is, when all measurements are available, written as $\mathbf{h}(\mathbf{x}) = \begin{bmatrix} x & y & z & \gamma & \kappa \end{bmatrix}$. Its size varies with the number of measurements available. The filter runs at 100 Hz to take into account the robot measurements.

To take into account the poor imaging quality of the 3D US probe, we propose to reset the covariance matrix of the measurement noise $\mathbf{R}$. Thus, the further the needle is from the US transducer, the poorer its visibility is and the higher the corresponding term is reset in $\mathbf{R}$.

When crossing the interface between two tissues of different elasticities, we expect the curvature of the needle path to change. The term corresponding to κ in the error covariance matrix $\mathbf{P}$ is therefore reset. This reflects a decreased trust in the current estimation.

B. Results

The system is composed of a robot holding the needle to insert it into a phantom (cf. Figure 2). The robot used for 24 Gauge Nitinol needle insertions has been developed for prostate brachytherapy [14]. The ultrasound volumes are acquired every second with a 3D end-fire probe 4DEC-9/10 used with the Ultrasonix Sonix RP ultrasound system. The US volume voxels are 0.4 mm^3 cubes. Pre-operative SWE measurements are taken into account.

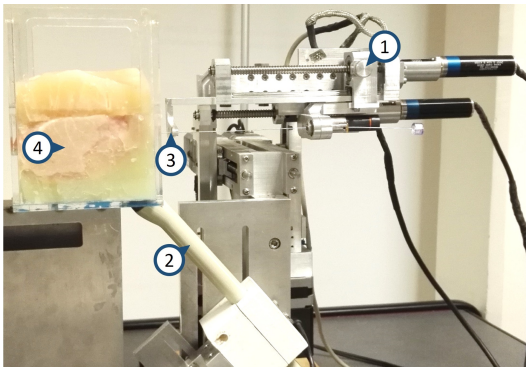

Fig. 2. Experimental setup composed of the Prosper Robot (1), 3D US imaging system (2), Beveled-tip needle (3) and Pork tissue incorporated in Agar (4) [1].

An example of needle tip path estimation is shown in Figure 3. The mean needle tip localization error was 0.6 ± 0.3 mm for 51 insertions made in both phantoms and biological tissues. This error is calculated as the distance with a manual segmentation. The observer also predicts the final tip pose with an error smaller than 2 mm after observing the first 2 cm of 8 cm long insertions. The asynchronous functioning of the filter along with its prediction precision provide a ROI that is robust to both elasticity change and needle disappearance. This greatly helps the needle tip tracking in noisy 3D US volumes especially when steering in heterogeneous tissues.

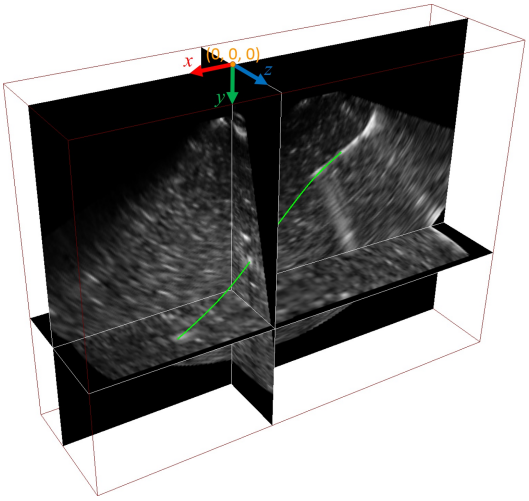

Fig. 3. 3D US volume of a needle inserted in an Agar phantom. The volume is represented by three planar sections. Estimated needle tip path represented by the green curve [1].

III. Conclusion

The multi-rate, multi-sensor compatible observer presented here benefits from all available measurements to provide a fine estimate of the needle tip pose and its path curvature. An adapted segmentation method, inherited from

[16], uses the resulting ROI for fine analysis of the 3D US volumes and for needle tip segmentation. The proposed filtering can also improve targeting. The good estimation of the tip behavior and its uncertainties could benefit adapted control laws and path planning methods.

REFERENCES

[1] G. Lapouge, J. Troccaz and P. Poignet, Multi-rate unscented Kalman filtering for pose and curvature estimation in 3D ultrasound-guided needle steering, Control Engineering Practice, Control Engineering Practice, vol. 80, pp. 116-124, 2018.

[2] J. Chevrie, A. Krupa, and M. Babel, Online prediction of needle shape deformation in moving soft tissues from visual feedback, International Conference on Intelligent Robots and Systems (IROS), IEEE/RSJ, pp. 2375-2380, 2016.

[3] J. Huang, J. K. Triedman, N. V. Vasilyev, Y. Suematsu, R. O. Cleveland, and P. E. Dupont, Imaging Artifacts of Medical Instruments in Ultrasound-Guided Interventions, Journal of Ultrasound in Medicine, vol. 26, no. 10, pp. 1303-1322, 2007.

[4] P. Moreira and S. Misra, Biomechanics-based curvature estimation for ultrasound-guided flexible needle steering in biological tissues, Annals of biomedical engineering, vol. 43, no. 8, pp. 1716-1726, 2015.

[5] M. Abayazid, P. Moreira, N. Shahriari, S. Patil, R. Alterovitz, and S. Misra, Ultrasound-guided three-dimensional needle steering in biological tissue with curved surfaces, Medical Engineering & Physics, vol. 37, no. 1, pp. 145-150, 2015.

[6] B. Fallahi, C. Rossa, R. S. Sloboda, N. Usmani, and M. Tavakoli, Sliding-based image-guided 3D needle steering in soft tissue, Control Engineering Practice, vol. 63, pp. 34-43, Jun. 2017.

[7] T. K. Adebar and A. M. Okamura, 3D segmentation of curved needles using doppler ultrasound and vibration, in International Conference on Information Processing in Computer-Assisted Interventions, 2013, p. 61-70.

[8] P. Mignon, P. Poignet, and J. Troccaz, Using rotation for steerable needle detection in 3D color-Doppler ultrasound images, International Conference on Engineering in Medicine and Biology Society (EMBC), IEEE, 2015, pp. 1544-1547.

[9] P. Chatelain, A. Krupa, and M. Marchal, Real-time needle detection and tracking using a visually servoed 3D ultrasound probe, International Conference on Robotics and Automation (ICRA), IEEE, 2013, p. 1676-1681.

[10] P. Chatelain, A. Krupa, and N. Navab, 3D ultrasound-guided robotic steering of a flexible needle via visual servoing , International Conference on Robotics and Automation (ICRA),IEEE, 2015, p. 2250-2255.

[11] P. Mignon, P. Poignet, and J. Troccaz, Automatic Robotic Steering of Flexible Needles from 3D Ultrasound Images in Phantoms and Ex Vivo Biological Tissue, Annals of Biomedical Engineering, vol. 46, no. 9, pp. 1385-1396, 2018.

[12] L. Armesto, S. Chroust, M. Vincze, and J. Tornero, Multi-rate fusion with vision and inertial sensors, International Conference on Robotics and Automation (ICRA), IEEE , 2004, vol. 1, p. 193-199.

[13] R. J. Webster, J. S. Kim, N. J. Cowan, G. S. Chirikjian, and A. M. Okamura, Nonholonomic Modeling of Needle Steering, The International Journal of Robotics Research, vol. 25, no. 5-6, p. 509-525, 2006.

[14] N. Hungr, M. Baumann, J.-A. Long, and J. Troccaz, A 3-D ultrasound robotic prostate brachytherapy system with prostate motion tracking, IEEE Transactions on Robotics, vol. 28, no. 6, pp. 1382-1397, 2012.

[15] M. Abayazid, R. J. Roesthuis, R. Reilink, and S. Misra, Integrating Deflection Models and Image Feedback for Real-Time Flexible Needle Steering, IEEE Transactions on Robotics, vol. 29, no. 2, pp. 542-553, 2013.

[16] H. Younes, S. Voros, and J. Troccaz, Automatic needle localization in 3D ultrasound images for brachytherapy, International Symposium on Biomedical Imaging (ISBI), IEEE, pp.1203-1207, 2018.